Int. J. Electrochem. Sci., 13 **(2018)** 5474 – 5487, doi: 10.20964/2018.06.57

International Journal of
ELECTROCHEMICAL
SCIENCE
www.electrochemsci.org

Self-sacrificed Synthesis of Amorphous Carbon-Coated SiO_x as Anode Materials for Lithium-Ion Batteries

Hao Cui[1], *Kai Chen*[2], *Yafei Shen*[2], *Zhao Wang*[1,*]

[1] State Key Laboratory Advance Technology for Materials Synthesis and Processing, School of Materials Science and Engineering, Wuhan University of Technology, 122, Luoshi Road, Wuhan, 430070, China.
[2] Wuhan Jingce Electronic Technology Co., Ltd. 55, Nanhu Road, Wuhan, 430070, China
[*]E-mail: wangzhao2070@126.com

Received: 10 February 2018 / *Accepted:* 6 April 2018 / *Published:* 10 May 2018

Amorphous carbon coated SiO_x is developed by the self-sacrifice of self-assembled Nafion/SiO_2 and explored as anode materials for lithium-ion batteries to overcome the sever pulverization and the resultant loss of specific capacity caused by the volume expansion of Si during the lithium ions insertion/extraction process. The amorphous carbon coated SiO_x (SiO_x/C) is prepared by using self-assembled Nafion/SiO_2 as the precursor, following by magnesium reduction of SiO_2 and carbonization of Nafion ionomers. XPS, TEM and XRD results indicate that most of SiO_x was reduced to amorphous Si^0 with small amount of Si^{2+} and Si^{4+}, which are coated by amorphous carbon. As the amorphous carbon coating can effectively reduce the volume change of SiO_x-based material during the charge-discharge process and enhance the electronic conductivity of the material, the Nafion-derived amorphous carbon coated SiO_x exhibits improved reversible capacity, better cycling stability and rate capability than that of pure amorphous carbon at Si loading below 10 wt%

Keywords: Self-sacrificed, amorphous carbon-coated, silicon/C, anode materials, lithium-ion battery

1. INTRODUCTION

Lithium-ion batteries(LIBs) are widely used in portable electronic products such as cell phones, laptops and digital cameras[1, 2] because of their high capacity, fast reversible charge-discharge, high coulomb efficiency and etc[3, 4]. With the advancement in science and technology, the extended application of LIBs from electronic terminal equipment to the field of electric vehicles technologies becomes an inevitable trend[5-7]. However, an increase of specific electrode capacity is required to achieve reasonable energy and power densities for these applications, which is by far still a challenge

for the lithium ion battery industry[8-10]. Thus, the development of novel electrode material is necessary to meet these challenges.

Currently, silicon has been considered as one of the most promising anode materials for the next-generation of LIBs because of its high theoretical specific capacity (4200 $mAhg^{-1}$, which is ten times higher than that of the commercial graphite, ~372 mAh g^{-1}[11], abundance reserves in earth and low working potential for lithium insertion and extraction (<0.5 V vs Li/Li^+)[12, 13]. However, several intrinsic drawbacks of silicon make it still far from commercialization as LIB anodes. Among them, the large volume expansion (>300%) in silicon anode during the lithium ions insertion/extraction process is considered to be one of the critical challenges. The volume expansion of silicon brings a cracking and cause a severe pulverization in silicon anode, which results in a rapid decrease in the specific capacity with rather low stable performance[14]. In addition, the large volume change also leads to the continuous formation of unstable solid electrolyte interphase (SEI), which consumes a considerable amount of electrolyte and lithium in Li-battery[15]. As a result, the side effect from the volume expansion of silicon has to be solved before its commercialization.

To overcome the volume expansion of Si during the lithium ions insertion/extraction process, researchers have done plenty of explorations on the route to decrease the stress generated from the volume expansion of silicon. Nano-structured Si electrodes is one of the potential solutions as nano-sized Si could accommodate the mechanical stain and shorten the transmission distance of lithium ions during lithiation and delithiation process[16]. As a result, nano-silicon with various morphology, including nanoparticles[17, 18], nanowires[19], nanotubes[20], porous silicon[21] were synthesized and studied as anode materials for LIBs. In addition, X.H. Liu [22] studied the lithiation of individual silicon nanoparticles in real time with an in situ transmission electromicroscopy and discovered a critical particle diameter (~150 nm), below which the particles neither cracked nor fractured upon first lithiation. Besides that, another effective way is to introduce conductive buffer matrixes (i.e., Si/amorphous C[23, 24], Si/graphene[25], Si/ conductive polymers[26]) that could highly improve the conductivity of silicon material and prevent the rapid loss in the capacity of LIBs[16]. However, the interaction between nano-silicon and carbon base is still a concern if one wants to synthesis Si/C with high cycle and rate performance. This has been confirmed by X. Zhou[27] who concluded that the physical mixed Si-rGO had low cycle and rate performance because of the lack of chemical bonding between Si and rGO.

Perfluorosulfonic polymers such as Nafion, which was constituted by a flexible and hydrophobic carbon main chain (i.e., -$[(CFCF_2)(CF_2CF_2)_m]$-) and large amount of side chains terminated with a hydrophobic -SO_3H group, i.e.,–$(OCF_2(CF_3)OCF_2CF_2SO_3H$, has been intensively studied as proton exchange membrane fuel cell[28]. Moreover, since the -SO_3H group in Nafion molecular are negatively charged (-SO_3^-) in aqueous condition, and the surficial charge of nano-oxides can be modified by adjusting the pH of preparation solution, electrostatic self-assembly method was developed by researchers to synthesize Nafion/nano-oxides composites, such as Nafion/SiO_2[29], Nafion/TiO_2[30], Nafion/CeO_2[31]. In the procedure of electrostatic self-assemble, the positively charged oxides precursors were coated by the flexible and negatively charged Nafion ionomers, resulting a small and uniform oxides particle size. For example, H. Tang[29] prepared Nafion/SiO_2

through a self-assembly process. The SiO_2 particles in the composite could be downsized to 2.8±0.5 nm due to the strong interaction between SiO_2 and Nafion limits the growth of SiO_2.

Since amorphous carbon usually are obtained by pyrolysis of polymer materials at high temperature, the strong interaction between Nafion and SiO_2 in the self-assembled Nafion/SiO_2 could offer a small SiO_2 size. More interestingly, Nafion is the ideal source for the in-situ formation of amorphous carbon coated silica. In this work, self-assembled Nafion/SiO_2 was used as the precursor for the synthesis of amorphous SiO_x/C anode material for LIBs and excellent electrochemical performance of the anode was demonstrated.

2. EXPERIMENTAL SECTION

2.1 Preparation of amorphous carbon coated SiO_x composite

In this study, Nafion-derived carbon coated SiO_x sample (SiO_x/C) with different Si loadings, including 2 wt%, 5 wt%, 7 wt%, 10 wt% and 15 wt% of Si, were prepared by self-sacrifice process, including: self-assembly process, thermal reduction of SiO_2 and carbonization of Nafion ionomers, as it was illustrated in Figure 1.

In detailed, Nafion/SiO_2 precursor was prepared through electronicstatic self-assembly process as described previously[29]. Briefly, Nafion ionomers (EW=1000, 5 wt% Nafion, DuPont, USA) were transferred to N-methyl-2-pyrrolidone (NMP, Fluka) solution by distilling a mixing solution containing 100 mL Nafion and 100 mL NMP till the mixture solution temperature reached 203 °C. Before the transferring, the pH of Nafion solution was adjusted to 7 with NaOH under magnetic stirring. Tetraethoxysilane (TEOS, Shanghai Reagent Co. Ltd.) was weighted and dissolved into 50 mL Nafion/NMP mixture using a homogenizer. Then, diluted HCl solution (37 wt% HCl, Shanghai Reagent Co. Ltd.) was dropped into the mixture under vigorous stirring. During this step, TEOS was expected to hydrolysis with nano SiO_2 formation. Meanwhile, positively charged nano SiO_2 was electronically adsorbed on the negatively charged $–SO_3$ sites of Nafion ionomers as it was presented in Figure 1. Self-assembled Nafion–SiO_2 precursor were obtained after the mixture was stirred for 8 h and dried overnight in a vacuum oven at 90 ^oC.

After that, the Nafion/SiO_2 precursor and metallic magnesium powder were uniformly mixed with a Si/Mg molar ratio of 1:2, and calcined at 650 °C for 4 h under nitrogen atmosphere with a heating rate of 5 $^oC\ min^{-1}$. After cooling down to room temperature (RT), the product was washed in 1 mol L^{-1} HCl solution for 12 h to remove MgO and separated from the liquid by centrifugation and subsequently washed with ultra-pure water and centrifuged (five times), followed by drying under vacuum at 80 ^oC for 24 h. After that, the solid product was transferred into quartz boat and heated to 900 °C under nitrogen atmosphere for 3h, with a heating rate 5 °C min^{-1}. Finally, SiO_x/C sample was obtained with different normal Si loading 2, 5, 7, 10 and 15 wt%. For comparison, the pure Nafion-derived carbon coating was prepared under the same procedure without TEOS as the reference.

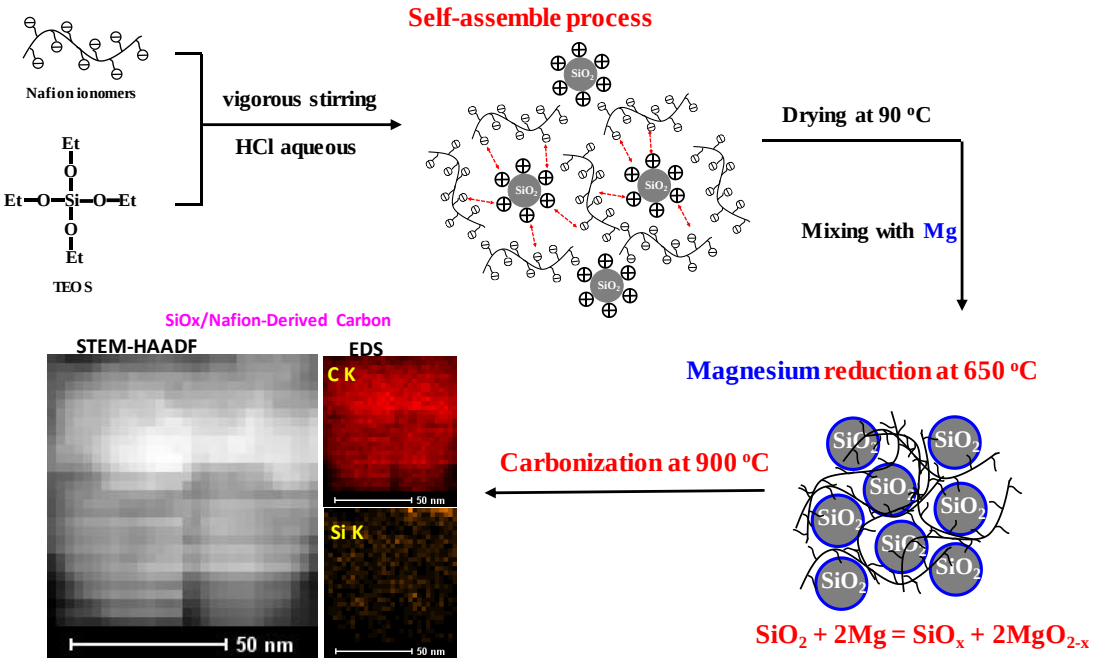

Figure 1. Scheme for the formation of the Nafion-derived carbon coated SiO_x. The inset shows the STEM-HAADF and EDS of SiO_x/C sample

2.2 Material characterizations

2.2.1 Physical characterizations

The crystal structure of all prepared samples was studied by a X-ray diffractometer (D8 Bruker Company) using the Cu Kα radiation (1.5418 Å; 40 kV and 15 mA) with the angle range of 10 - 80º under air. The morphology of prepared samples was imaged by transmission electron microscopy (TEM, JEM-2100F, Japan) operating at 200 kV and statistical analysis of the SiO_x particle size distribution (PSD) in SiO_x/C samples was obtained by counting more than 100 particles, using the software Image J. The average particle diameter was deduced from the equation $d_m=\Sigma n_i d_i^3/\Sigma n_i d_i^2$ where n_i is the number of the particles of diameter d_i. The state of carbon was analyzed by Raman spectrometer (Raman, In Via, RENISHAW, 514.5 nm wavelength) and X ray photoelectron spectroscopy (XPS, Thermo Scientific ESCALAB 250Xi, Al Ka, 1486.6 E) was employed in obtaining the further information abut C_{1s} and Si_{2p}. The decomposition behavior of the samples was analyzed by the thermogravimetric analysis (TGA, a Seiko 320 thermobalance) under air (20 mL min^{-1}) from room temperature to 800 ^oC with a heating rate of 15 °C min^{-1}.

2.2.2 Electrochemical characterizations

The electrochemical properties of all samples were tested using coin cell (CR2016), which was assembled in the glove box protected by argon.

As for the assemble of coin cell, a mount of weighed carboxymethyl cellulose（CMC） was firstly poured into a small beaker of water and stirred vigorously for 10 h to homogeneity. SiO_x /C composite and acetylene black were mixed by grinding dish for 1 h. Then the mixture was added to the CMC solution under magnetic stirring for 10 hours to prepare a slurry, which contains SiO_x/C composite: acetylene black: CMC = 6: 3: 1. Then, the slurry was coated with a predetermined thickness on the pre-cleaned copper foil, and dried in a vacuum oven at 120 ^oC for 24 h. The electrolyte was 1 M $LiPF_6$ in ethylene carbonate (EC)/ ethylmethyl carbonate (EMC)/ dimethyl carbonate (DMC) with a volume ratio of 1:1:1, the counter electrode was lithium metal and the separator membrane was a celgard 2400 microporous polypropylene.

The electrochemical performance of the as-prepared SiO_x/C were studied by galvanostatic charge-discharge cycling tests and electrochemical impedance spectroscopy (EIS) with the pure carbon coating as a reference. Galvanostatic charge/discharge cycles and rate performance were tested at different current densities on a Land battery test system in the voltage region between 0.01 and 2 V. The EIS was tested with the frequency range from 0.01 Hz to 106 Hz and the voltage amplitude of 5 mV at open circuit potential (OCP).

3. RESULTS AND DISCUSSION

3.1 The physical properties of the materials

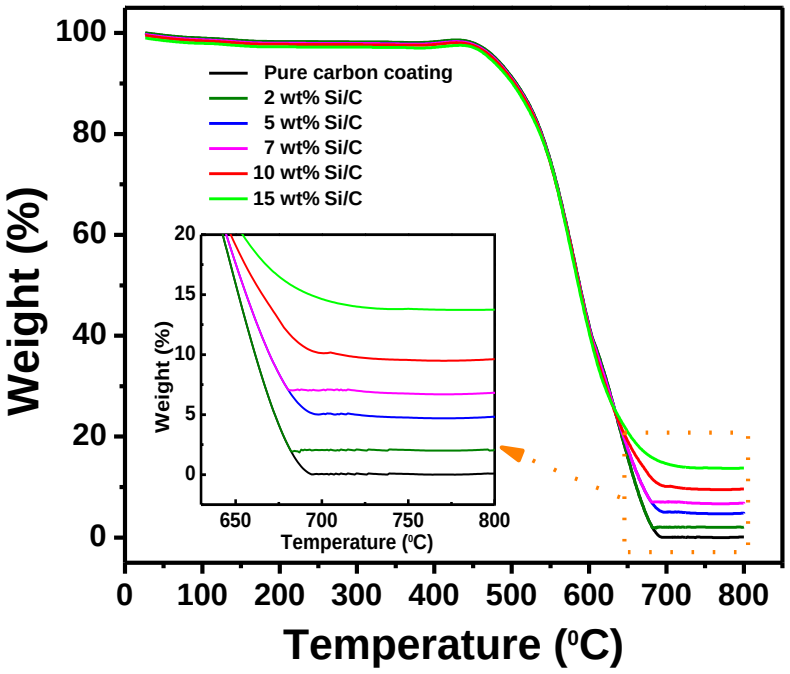

Figure 2. Thermogravimetric analyses was performed on the prepared SiO_x/C sample with different Si loadings;

As confirmed by TGA analyzation (Figure 2), the pure carbon coating can be fully oxidized and its weight percentage decreased rapidly from ~100% to 0 in the temperature range between 400 and 700 ^{o}C under air, thus the silicon loading in SiO_x/C samples could be evaluated by TGA method. It can be seen that the weight loss of the rest SiO_x/C samples between 400 and 700 °C was resulted from the combustion of carbon coating, and it agrees with the TGA curve of the pure Nafion-derived carbon reference. The silicon loading in the Si/C samples determined by the residual mass was highly consistent with the expected Si loading (2, 5, 7 10 and 15 wt%, respectively).

Figure 3 shows the X-ray diffraction (XRD) patterns of all the SiO_x/C samples. The pure carbon coating only show two broad peaks, 26.0° and ~43.0°, which are assigned to the (002) and (101) plane of carbon (JCPDS: 65-6212)[23, 25], respectively. The large full width at half maximum (FWHM) indicates that the carbon coating mainly existed in amorphous form. After introducing Si to carbon coating, with loading increased from 2 to 15 wt%, Figure 3 shows that they have similar XRD curves, which was similar to the pure carbon coating. Besides that, no detailed crystal information about SiO_x can be observed, and it means that either the particle size of silica was too small to be recognized by XRD or the phase of SiO_x was also amorphous. As a result, further characterization need to be carried on the samples.

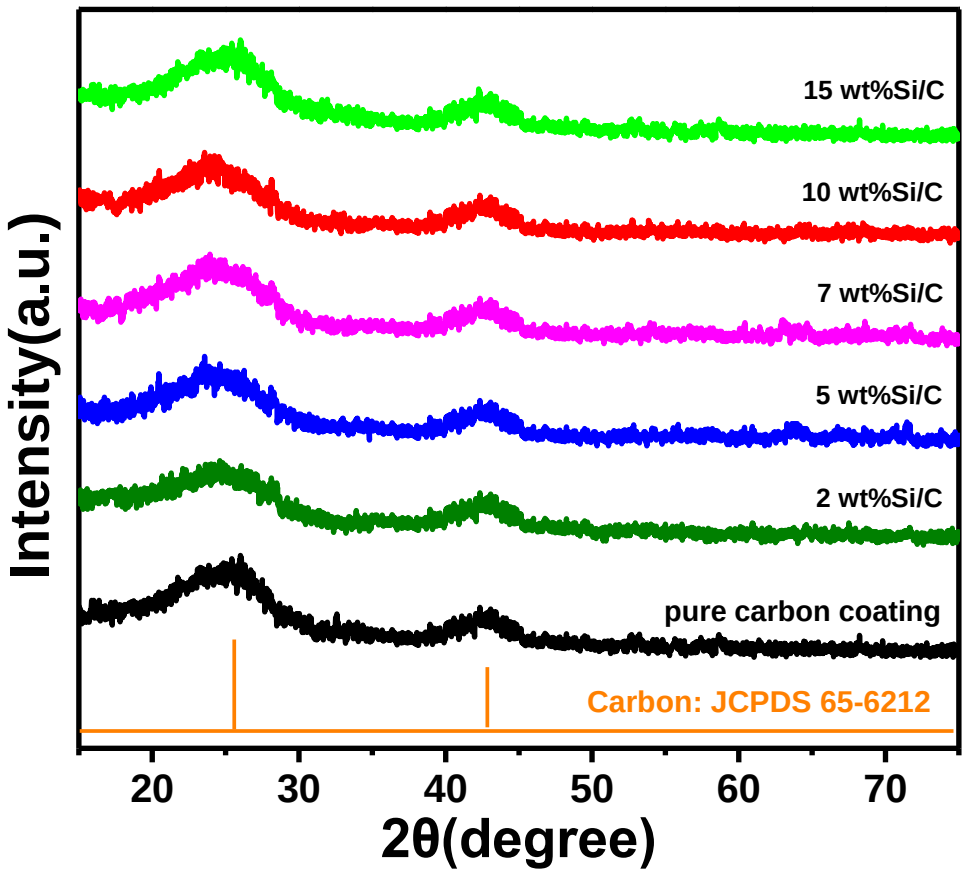

Figure 3. XRD of the prepared SiO_x/C sample with different Si loadings

The structure of the carbon coating in all samples was further analyzed by Raman spectra (Figure 4). In Figure 4, all samples show two main peaks: 1350 cm^{-1}（D-bond）and 1590 cm^{-1} (G-band). Since the strong peak at ~1350 cm^{-1} (D-bond) is associated with the amorphous carbon materials[32], while the weak peak at ~1590 cm^{-1} (G-band) is attributed to the vibration of sp^2-bonded carbon atoms in a 2D hexagonal lattice[33]. In addition, absence of 2D peak, which is an character peak of graphite structure, also indicate that the carbon coating support are composed of two structures of sp^2 and sp^3 hybrids, which implies these samples have low graphitization degrees.

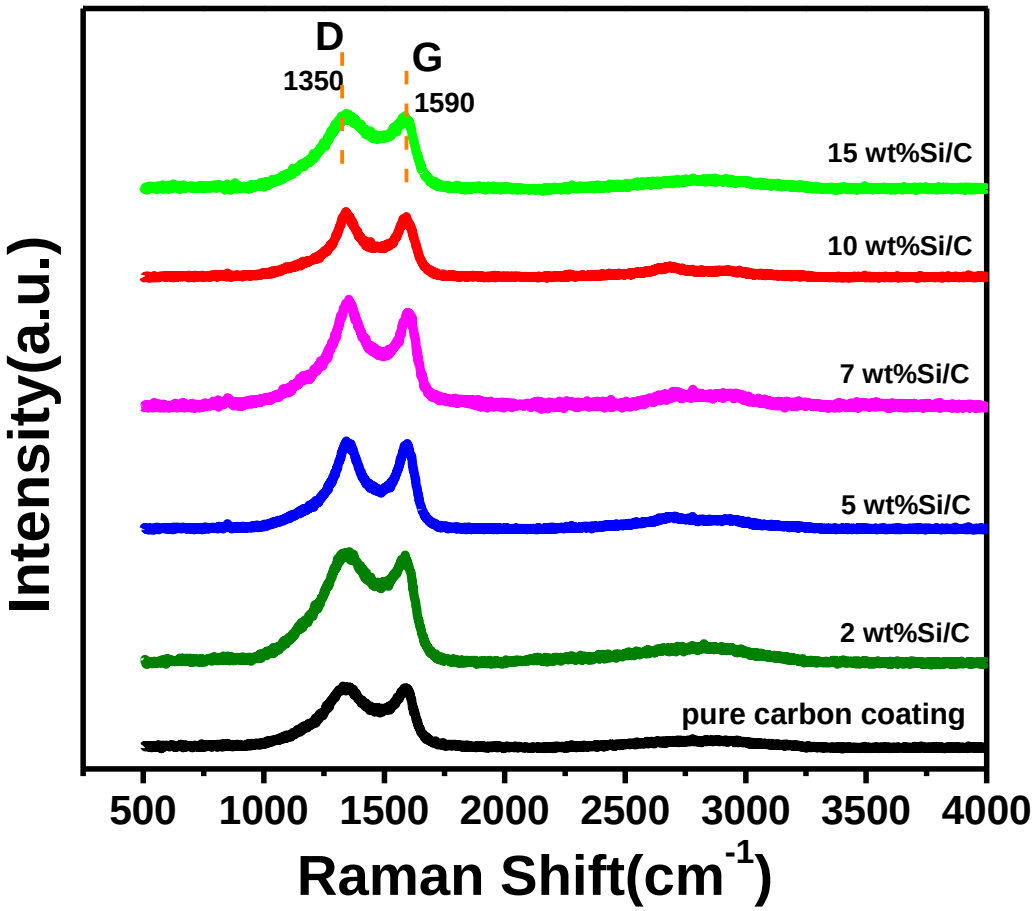

Figure 4. Raman of the prepared SiO_x/C sample with different Si loadings.

To obtain further information about the morphology of the carbon coating and SiO_x, TEM technique was applied on all SiO_x/C samples (Figure 5), with pure carbon coating as reference. The carbon coating is transparent while dark points are amorphous SiO_x. It can be found that SiO_x particles were coated by the amorphous carbon in all SiO_x/C samples. As presented in the inset of Figure 5, the particle size of silica are similar, ~75 nm. Besides that, combing with the XRD results (Figure 3), it allows to conclude that the SiO_x component in SiO_x/C samples was amorphous.

The chemical states of the samples were further evaluated by X-ray photoelectron spectra (XPS) spectrum (Figure 6). Compared with the pure carbon coating reference, Figure 6a shows that all

SiO_x/C samples contain F, O, N, C, S and Si elements, the characteristic binding energy of which were 685.7, 531.8, 398.4, 285.8, 164.3 and 100.1 eV, respectively[34]. Heteroatoms such as F, S and N may be from the unevaporated Nafion residual during carbonization thermal treatment in N_2, while O may come from the adsorbed oxygen on the samples and in SiO_x. In Figure 6b-f, The peak belongs to SiO_x component can be divided into Si^0 (99.8 eV), Si^{2+} (101.8 eV), Si^{4+} (103.6 eV), which was also observed in previous study[35].

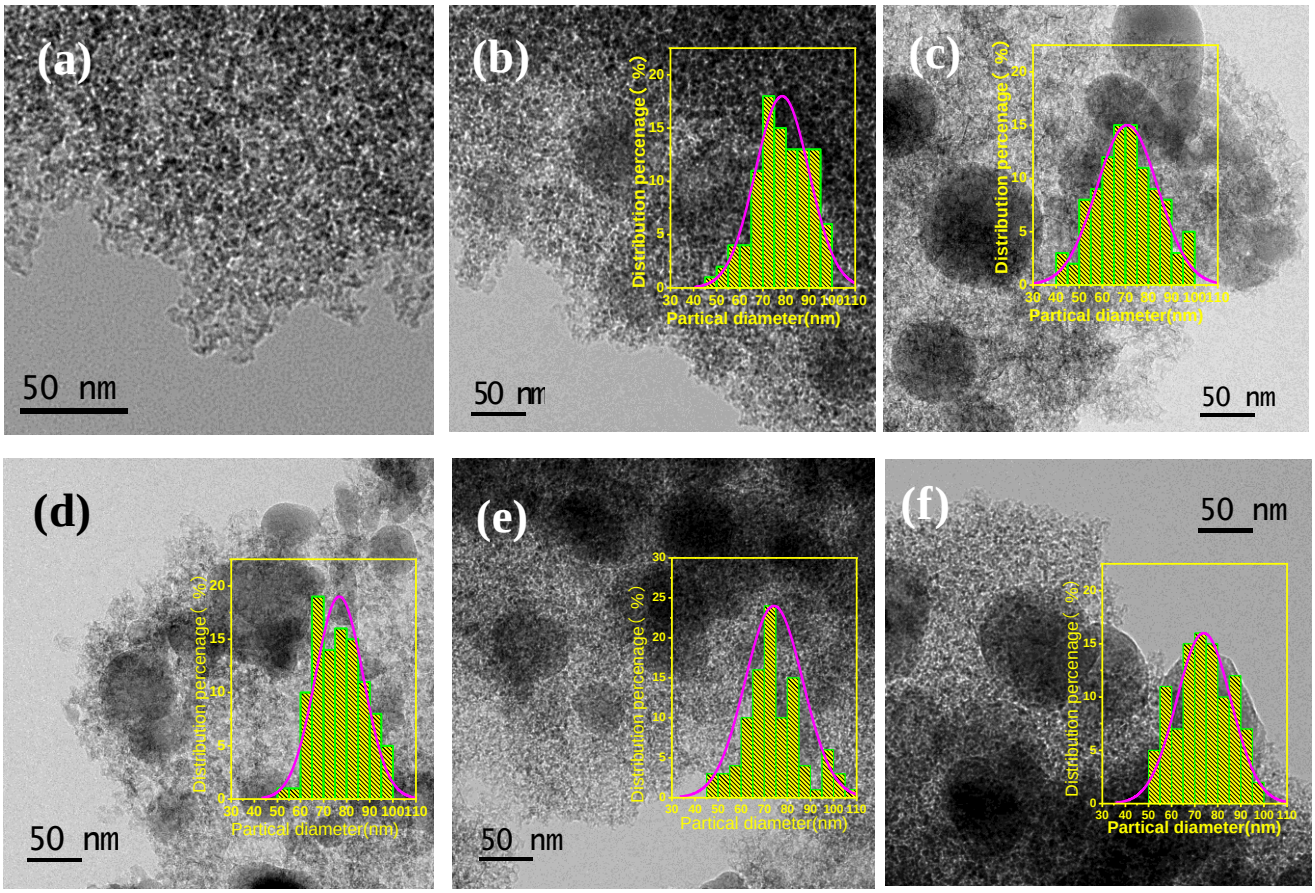

Figure 5. TEM of the pure carbon coating (a) and the prepared SiO_x/C sample with different Si loadings: 2 wt% (b), 5 wt% (c), 7 wt% (d), 10 wt% (e), 15 wt% (f).

In addition, the main peak corresponded to Si^0 and other two peaks (i.e., Si^{2+}, Si^{4+}) with weak intensity also indicates the fact that Si^0 was the main phase existed in all SiO_x/C samples. Moreover, the C peaks of all samples can be divided into three peaks: 284.7, 286.3 and 288.2 eV, corresponding to C-C, C-O and C=O groups, respectively (Figure 6g-l). Most of C component in all samples stayed in the form of C-C bond, and only a small number of hydroxyl groups on the surface. The XPS results show a direct evidence that the formation of SiO_x and amorphous C.

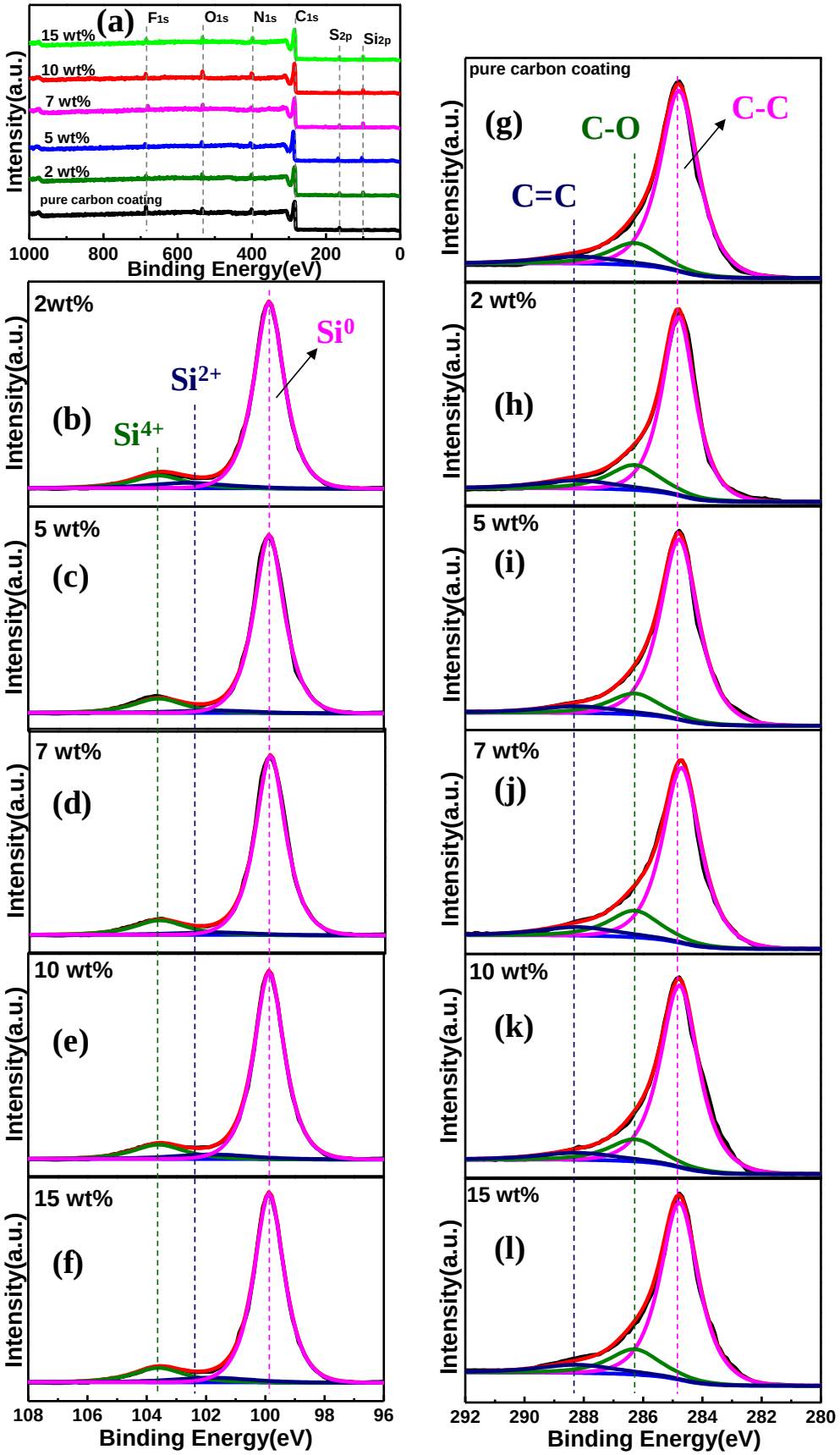

Figure 6. XPS spectra and curve-fitted peak components of pure carbon coating and all SiO_x/C samples with different Si loadings: (a) Survey spectra; (b-f) High resolution Si_{2p} spectra; (g-l) High resolution C_{1s} spectra.

3.2 Electrochemical performance of the materials

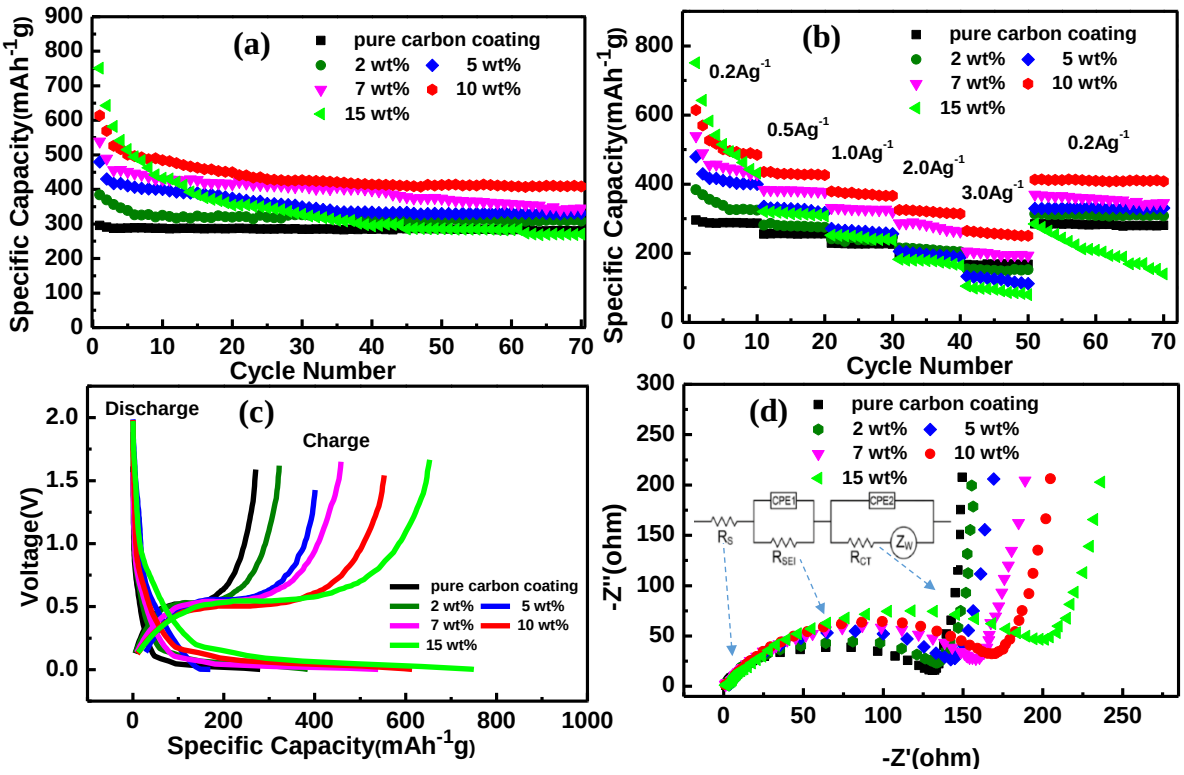

Figure 7. Electrochemical properties of SiO_x/C samples with different Si loadings: (a) the cycling property at 0.2 A g^{-1}, (b) the rate performance at different current densities, (c) First charge-discharge curves at 0.2 A g^{-1} and (d) the electrochemical impedance plots of all the SiO_x/C composites.

The stability of the SiO_x/C samples as anode material for LIBs was evaluated by the cycling performance, which was tested by a repetition of discharging and charging process between 0.01 and 2 V at a current density of 0.2 A g^{-1} for 70 cycles, shown in Figure 7a. The pure carbon coating reference shows the lowest initial specific capacity of 295.5 mAh g^{-1}, which slightly decreased to around 280 $mAhg^{-1}$ after 70 cycles. As for SiO_x/C samples, the initial specific capacity increased gradually from 384.1 to 750.5 mAh g^{-1} with Si loading changed from 2 to 15 wt%. It indicates that the addition of amorphous SiO_x could largely improve the initial capacity of carbon coating materials as the high theoretical specific capacity of pure silicon (4200 mAh g^{-1}). Besides that, the addition of Si decreases the stability of carbon coating (Figure 7a) as may be caused by the large volume evolution (>300%) of SiO_x during charge-discharge process. However, interestingly, the balance between the specific capacity and stability of the anode could be achieved at silicon loading staying lower than 10 wt%. Specially, for SiO_x/C with 10 wt% Si, the specific capacity was ~614.5 mAh g^{-1} at the beginning of cycling test. During the stability test for 70 cycles, it decreased gradually to ~410 mAh g^{-1}, which is still much higher than the initial capacity of the pure carbon coating.

Figure 7b reveals the rate capability of the SiO_x/C samples at different current densities of 0.2, 0.5, 1, 2 and 3 A g^{-1} between 2.0 and 0.01 V versus Li^+/Li for 10 cycles, with the pure carbon coating as a reference. At low current desity, i.e., 0.2 A g^{-1}, the discharge capacity of the cells based on the pure carbon coating and the SiO_x/C with different Si loadings (2, 5, 7, 10 and 15 wt%) anode at 0.2 A g^{-1} was 286.9, 324.8, 399.7, 428.8, 431.4 and 432.1 mAh g^{-1} after 10 cycles, respectively, similar as it was observed in Figure 7a. With an increase of the current density from 0.2 to 3.0 A g^{-1}, the reversible capacity decreased gradually. For example, the initial specific capacity of SiO_x/C with 10 wt% Si sample are 614.2, 435.7, 378.6, 325.4 at 264.4 for the test at current densities of 0.2, 0.5, 1, 2 and 3 A g^{-1}, respectively. However, for all the samples, the specific capacity becomes more stable with the increase of current density, and SiO_x/C samples show a higher capacity than that of the pure carbon coating at 3 A g^{-1}. It mainly because the amorphous carbon can withstand more external stress, the internal structure becomes very loose, and abundant internal voids can provide sufficient space for the volume change of SiO_x when SiO_x reacts with lithium ions to produce volume change. Meanwhile, such a composite structure facilitates infiltration of the electrolyte and shortens the ion transport distance. As a result of these favorable features, the sample exhibits higher lithium storage capacity and stability at high current densities. When the charge-discharge current returned to 0.2 A g^{-1} again, all SiO_x/C samples maintained a good stability in 51~70 cycles. Exceptionally, the battery with 15 wt% SiO_x/C anode shows a serious decay from ~300 to 150 mAh g^{-1} as maybe the destroyed anode structure resulted in a rapid decline for lithium storage capacity. As a result, it allows to conclude that, at Si loading lower than 10 wt%, the rather high stable specific capacity of SiO_x/C samples is explained by the protection and promotion effect of the amorphous carbon coating.

Figure 7c shows the first charge and discharge curves of the SiO_x/C composites at a current density of 200 mA g^{-1}. The first discharge capacities (lithium ion insertion) of battery containing SiO_x/C anode materials with different Si loadings, 0, 2, 5, 7, 10 and 15 wt% Si are around 295.5, 384.1, 479.5, 538.9, 614.5 and 750.5 mAh g^{-1}, respectively, meanwhile, the first charge capacity (lithium ion extraction process) were around 270, 322.3, 400.7, 458.1, 553.9 and 653.5 mAh g^{-1}, respectively. The first irreversible capacity of SiO_x/C composites is mainly due to the decomposition of the electrolyte and the formation of a solid electrolyte membrane on the electrode surface.

Table 1. Impedance parameters for the SiO_x/C electrode with different Si loadings after 70th cycles

Silicon loading / wt%	R_S/Ω	R_{SEI}/Ω	R_{CT}/Ω
0	5.332	130.8	70.39
2	5.673	134.3	72.75
5	6.014	142.6	75.48
7	6.132	152.4	78.52
10	6.374	168.7	83.33
15	7.019	198.3	92.71

To further investigate the effect of additional SiO_x on the electrochemical impedance of the carbon coating, all Li-battery cells were tested by electrochemical impedance spectroscopy (EIS) measurement after 70th cycling test (Figure 7d) with detailed data summarized in Table 1. According to the model of equivalent circuit (inset in Figure 7d), the resistance existed in Li-battery can be divided into three sections[36-38]: the internal contact resistance (R_S), the ionic diffusion resistance of Li^+ (R_{ESI}) and the charge transfer impedance (R_{CT}). Meanwhile, the CPE_1 and CPE_2 represent the capacitance of the SEI layer and the electrode/electrolyte, respectively. The Z_w is the Warburg diffusion impedance from the lithium diffusion process[39]. As it was reflected in ESI Nyquist curves, the semicircle part of high frequency x-intercept corresponds to the R_S, the mid-frequency semicircle responds to the R_{SEI} and the oblique line of the low frequency region is mainly related to R_{CT}. In Table 1, the pure carbon coating shows that R_S was around 5.332 Ohm, with R_{SEI} ~130.8 Ohm and R_{CT} ~70.39 Ohm. The R_S of SiO_x/C samples was similar to that of the pure carbon coating. Besides that, SiO_x/C samples have higher R_{SEI} and R_{CT} than that of the pure carbon coating. The higher Si loading, the larger are R_{SEI} and R_{CT} as included in Table 1. It means that the addition of Si component hinders the Li^+ ionic diffusion in SEI layer and the charge transfer in the electrode/electrolyte interphase.

Table 2. Comparison of the electrochemical properties of the SiO_x/C materials with earlier reported anode materials for Li-battery

Anode materials	Si loading / wt%	Initial discharging capacity / mAh g^{-1}	Initial charging capacity / mAh g^{-1}	Initial coulombic efficiencies / %	Final capacity / mAh g^{-1}	Capacity retention after 70 cycles /%	Ref
SiO_2@graphene aerogel	55.9	1042.7	453.3	43.5%	~300	28.8	[40]
SiO_2/C fibers	22.1	~750	500	66.7%	465	62	[41]
SiO_x@C nanorods	41.8	1324	906	68.4%	700	52.8	[42]
Si/SiO_2@C	80	1763.4	1001.9	56.8	~510	28.9	[43]
SiO_x/C with different Si loadings	0	295.5	270	91.4	280	94.7	This work
	2	384.1	322.3	83.9	308.2	80.2	This work
	5	479.5	400.7	83.6	331.4	69.1	This work
	7	538.9	458.1	85.0	345. 8	64.2	This work
	10	614.5	553.9	90.1	408.5	66.5	This work
	15	750.5	653.5	87.1	270.1	36	This work

The electrochemical performance of SiO_x/C based batteries were summarized in Table 1, which also includes some previous similar studies focused on silica/carbon anode materials. Comparison with

previous study, the low initial capacities (<750 mAh g^{-1}) obtained in our study were mainly due to the rather low silica loadings (<15 wt%). However, Si/C samples exhibit a much higher coulombic efficiencies (>80%) as maybe the self-sacrificed process of Nafion molecular provides a high SiO_x particle dispersion with close interaction between C and SiO_x. It was also verified by the similar electrochemical impedance between SiO_x samples and C base (Table 1). Besides that, from the capacity retention after 70 cycles (Table 2), SiO_x coated by the amorphous carbon derived from Niafion (SiO_x/C) performed in this study also shows a higher cycles retention (>60%) than the previous similar study that focused on SiO_x/C materials. For example, the capacity of SiO_2@graphene aerogel based Li battery only has ~28.8% capacity retention, which is twice lower than that presented in this study.

4. CONCLUSION

In this paper, amorphous carbon coated SiO_x is prepared through a facile self-sacrificed synthesis approach and used as anode material for Lithium-ion batteries. The experimental Si loadings in the SiO_x/C samples, as verified by TG test, are highly in agreement with the theoretical value, demonstrating the high efficiency of the approach. XRD and Raman measurements reveals that the carbon base that derived by Nafion carbonization was amorphous. Combining with TEM, XRD and XPS, it can be concluded that most of SiO_2 was reduced to Si^0, with small amout of Si^{2+} and Si^{4+} formation, through the magnesium reduction treatment, and the SiO_x was also mainly stays in amorphous. As for the electrochemical property, SiO_x/C show slightly higher electrochemical impedance than that of pure carbon coating, but the addition of Si brings a larger reversible capacity, better cycling stability and higher rate capability than pure carbon when Si loading is no more than 10 wt%. The present results demonstrate the promises of the self-assembled SiO_x/C composite for lithium-ion batteries applications.

However, the particle size of SiO_x is slightly large (i.e., ~75 nm in 10 wt% Si/C), further work could be explored on the preparation of Nafion-derived carbon coated SiO_x with high Si loading and small particle size, which might show a rather high stability performance.

ACKNOWLEDGEMENT
This work was financially supported by the National Nature Science Foundation of China (51472187).

References

1. Z. Zhang, Q. Li, K. Zhang, W. Chen, Y. Lai, J. Li, *J. Power Sources*, 290 (2015) 159.
2. Y. Wang, H. Y. Liu, K. Wang, S. Q. Song, P. Tsiakaras, *Appl. Catal. B-Environ*, 210 (2017) 57
3. Y. Wang, X. Wen, J. Chen, S. Wang, *J. Power Sources*, 281 (2015) 285.
4. H.-C. Tao, L.-Z. Fan, X. Qu, *Electrochim Acta*, 71 (2012) 194.
5. D. Wang, Y. Min, Y. Yu, B. Peng, *J. Colloid Interf Sci*, 417 (2014) 270.
6. Q. Si, M. Matsui, T. Horiba, O. Yamamoto, Y. Takeda, N. Seki, N. Imanishi, *J. Power Sources*, 241 (2013) 744.
7. S. Cai, Z. Meng, H. Tang, Y. Wang, P. Tsiakaras, *Appl. Catal. B-Environ*, 217 (2017) 477.
8. X. Liu, D. Chao, Y. Li, J. Hao, X. Liu, J. Zhao, J. Lin, H. Jin Fan, Z. Xiang Shen, *Nano Energy*, 17 (2015) 43.

9. A. Marzouk, P.B. Balbuena, F. El-Mellouhi, *Electrochim Acta*, 207 (2016) 301.
10. I.S. Amiinu, X. Liu, Z. Pu, W. Li, Q. Li, J. Zhang, H. Tang, H. Zhang, S. Mu, *Adv. Funct. Mater.*, 28 (2018) 1704638-n/a.
11. S.R. Gowda, V. Pushparaj, S. Herle, G. Girishkumar, J.G. Gordon, H. Gullapalli, X. Zhan, P.M. Ajayan, A.L.M. Reddy, *Nano Lett*, 12 (2012) 6060.
12. L. Yue, H. Zhong, D. Tang, L. Zhang, *J. Solid State Electr.*, 17 (2013) 961.
13. O. Majoulet, C. Salameh, M.E. Schuster, U.B. Demirci, Y. Sugahara, S. Bernard, P. Miele, *Chem. Mater.*, 25 (2013) 3957.
14. Y.H. Sehlleier, S. Dobrowolny, I. Plümel, L. Xiao, F. Mahlendorf, A. Heinzel, C. Schulz, H. Wiggers, *J. Appl. Electrochem.*, 46 (2016) 229.
15. C. Ma, C. Ma, J. Wang, H. Wang, J. Shi, Y. Song, Q. Guo, L. Liu, *Carbon*, 72 (2014) 38.
16. N. Liu, H. Wu, M.T. McDowell, Y. Yao, C. Wang, Y. Cui, *Nano Lett*, 12 (2012) 3315.
17. K. Feng, W. Ahn, G. Lui, H.W. Park, A.G. Kashkooli, G. Jiang, X. Wang, X. Xiao, Z. Chen, *Nano Energy*, 19 (2016) 187.
18. H.-C. Tao, L.-Z. Fan, Y. Mei, X. Qu, *Electrochem. Commun.*, 13 (2011) 1332.
19. L.-F. Cui, R. Ruffo, C.K. Chan, H. Peng, Y. Cui, *Nano Lett*, 9 (2009) 491.
20. Z. Wen, G. Lu, S. Mao, H. Kim, S. Cui, K. Yu, X. Huang, P.T. Hurley, O. Mao, J. Chen, *Electrochem. Commun.*, 29 (2013) 67.
21. M. Ge, J. Rong, X. Fang, A. Zhang, Y. Lu, C. Zhou, *Nano Res.*, 6 (2013) 174.
22. X.H. Liu, L. Zhong, S. Huang, S.X. Mao, T. Zhu, J.Y. Huang, *Acs Nano*, 6 (2012) 1522.
23. J.-K. Lee, M.C. Kung, L. Trahey, M.N. Missaghi, H.H. Kung, *Chem. Mater.*, 21 (2009) 6.
24. H. Tang, Y. Zeng, D. Liu, D. Qu, J. Luo, K. Binnemans, D.E. De Vos, J. Fransaer, D. Qu, S.-G. Sun, *Nano Energy*, 26 (2016) 131.
25. X. Zhao, C.M. Hayner, M.C. Kung, H.H. Kung, *Adv. Energy Mater.*, 1 (2011) 1079.
26. C. Wang, H. Wu, Z. Chen, M.T. McDowell, Y. Cui, Z. Bao, *Nature Chemistry*, 5 (2013) 1042.
27. X. Zhou, Y.-X. Yin, L.-J. Wan, Y.-G. Guo, *Chem. Commun.*, 48 (2012) 2198.
28. K.A. Mauritz, R.B. Moore, *Chem. Rev.*, 104 (2004) 4535.
29. H. Tang, Z. Wan, M. Pan, S.P. Jiang, *Electrochem Commun*, 9 (2007) 2003.
30. W. Zhengbang, H. Tang, P. Mu, *J. Membrane Sci.*, 369 (2011) 250.
31. Z. Wang, H. Tang, H. Zhang, M. Lei, R. Chen, P. Xiao, M. Pan, *J. Membrane Sci.*, 421 (2012) 201.
32. M. Feng, J. Tian, H. Xie, Y. Kang, Z. Shan, *J. Solid State Electr.*, 19 (2015) 1773.
33. X. Bai, Y. Yu, H.H. Kung, B. Wang, J. Jiang, *J. Power Sources*, 306 (2016) 42.
34. H. Wu, G. Zheng, N. Liu, T.J. Carney, Y. Yang, Y. Cui, *Nano Lett*, 12 (2012) 904.
35. Y. Yu, L. Gu, C. Zhu, S. Tsukimoto, P.A. van Aken, J. Maier, *J. Adv. Mater.*, 22 (2010) 2247.
36. T. Wang, F. Wang, H. Zhu, *Mater Lett*, 161 (2015) 89.
37. Z. Zhou, Y. Xu, M. Hojamberdiev, W. Liu, J. Wang, *J. Alloy. Compd.*, 507 (2010) 309.
38. Y. Yao, M.T. McDowell, I. Ryu, H. Wu, N. Liu, L. Hu, W.D. Nix, Y. Cui, *Nano Lett*, 11 (2011) 2949.
39. J. Lai, H.-j. Guo, X.-q. Li, Z.-x. Wang, X.-h. Li, X.-p. Zhang, S.-l. Huang, L. Gan, *T. Nonferr. Metal. Soc.*, 23 (2013) 1413.
40. J. Meng, Y. Cao, Y. Suo, Y. Liu, J. Zhang, X. Zheng, Electrochim. Acta, 176 (2015) 1001.
41. Y. Ren, Y. Bo, H. M. Wei, J. N. Ding, Solid State Ion., 292 (2016) 27.
42. Y. Ren, M. Li, *J. Power Sources*, 306 (2016) 459.
43. Y. Zhou, Z. Tian, R. Fan, S. Zhao, R. Zhou, H. Guo, Z. Wang, *Powder Technol*., 284 (2015) 365.